Available online at www.sciencedirect.com

ScienceDirect

materialstoday: PROCEEDINGS

Materials Today: Proceedings 2S (2015) S466 – S473

Joint 3rd UK-China Steel Research Forum & 15th CMA-UK Conference on Materials Science and Engineering

Modelling of Secondary Dendrite Arms Evolution during Solidification by a Phase-field Method

Qi-Wei Zheng [a], Tao Jing [a,*], Hong-biao Dong [a,b]

[a]*School of Materials Science and Engineering, Key Laboratory for Advanced Materials Processing Technology, Ministry of Education, Tsinghua Unveristy, Beijing 100084, China*

[b]*Department of Engineering, University of Leicester, Leicester, LE1 7RH, UK*

Abstract

Mechanical property of cast metals is strongly dependent on solidification structure, in particular the secondary dendrite arms spacing. In this study a Phase Field Method was used to simulate the evolution of dendritic structure with coupled heat and solute diffusion during solidification. Coarsening and remelting of the secondary arms were simulated. It is found that (1) the base of the secondary arms doesn't decrease as coarsening theory predicts and the arms spacing keeps unchanged when the arm grows into a steady state, but the volume of the arms increases; (2) both remelting of secondary arms and coarsening of secondary arms can be observed, which agrees with the coarsening theory and experiment observations.

Selection and Peer-review under responsibility of the Chinese Materials Association in the UK (CMA-UK).

Keywords: Solidification, Phase Field Method, secondary dendrite arm, modelling of solidification

1. Introduction

Mechanical property of cast metals is strongly dependent on solidification structure, in particular the secondary dendrite arms spacing[1-3]. Many experimental investigations have revealed that the smaller the secondary arm spacing, the higher the strength of the as-cast metals[4]. Although many efforts have been focused on the

* Corresponding author. Tel.: +86-10-62785854.
E-mail address: jingtao@mail.tsinghua.edu.cn

Selection and Peer-review under responsibility of the Chinese Materials Association in the UK (CMA-UK).
doi:10.1016/j.matpr.2015.05.063

mechanism of the secondary aim spacing during solidification, there is no convincing mechanism to explain the spacing. In this study a Phase Field Method was used to simulate the evolution of dendritic structure with coupled heat and solute diffusion during solidification. Mechanism for spacing, including coarsening and remelting of the secondary arms will be reported.

1. Description of Phase Field Model

The phase-field model we used in our paper is based on the model proposed by Karma[5], in which both heat and solute diffusion are considered, so this method was applied to study the solute distribution in the solidification of a binary alloy in different thermal condition.

In Karmar's phase-field method, a continuous variable ϕ is introduced in to denote the local phase state. The variable is called phase-field variable or order parameter, and the value for each phase state can be assigned artificially. In our calculation we use ϕ=-1 for liquid phase while ϕ=1 indicates solid phase. Then the transition of ϕ from -1 to 1 indicates a solid-liquid interface.

The calculation of ϕ is governed by Allen–Cahn equation, which is the phase-field equation for non-conserved variable. The variable evolves to minimize the total free energy *F*.

$$\frac{\partial \phi}{\partial t} = -M \frac{\delta F}{\delta \phi} \tag{1}$$

The free energy consists of bulk free energy and interfacial energy introduced by the phase gradient. The bulk free energy f_{AB} is a function of local temperature, solute and ϕ. And it's the double-well function which has minimum at solid phase and liquid phase. The interfacial energy depends on the interfacial width *w* and the gradient of ϕ, and it controls the diffuse interface in the calculation. So the total free energy in the system can be written as:

$$F(\phi, c, T) = \int dV \left[\frac{w}{2} |\nabla \phi|^2 + f_{AB}(\phi, c, T) \right] \tag{2}$$

Then we can get the control equation for ϕ. In 2-Dimensional calculation the equation becomes :

$$\begin{aligned} &\tau(\vec{n}) \frac{\partial \phi}{\partial t} = [\phi - \lambda(u + Mc)(1-\phi^2)](1-\phi^2) \\ &+\nabla \cdot [w(\vec{n})^2 \nabla \phi] + \frac{\partial}{\partial x}[|\nabla \phi|^2 w(\vec{n}) \frac{\partial w(\vec{n})}{\partial \phi_x}] + \frac{\partial}{\partial y}[|\nabla \phi|^2 w(\vec{n}) \frac{\partial w(\vec{n})}{\partial \phi_y}] \end{aligned} \tag{3}$$

In the equation, λ is a coupling constant, *u* is dimensionless temperature, *m* is dimensionless liquidus slope. To involve anisotropy into the equation, we define interface width $\boldsymbol{w}$ and phase mobility constant $\boldsymbol{\tau}$ as

$$w(\vec{n}) = w_0 a_s(\vec{n}) \quad \tau(\vec{n}) = \tau_0 a_s^2(\vec{n}) \tag{4}$$

If we take $\boldsymbol{w}_0 = d_0\lambda/a_1$ as the unit length and $\boldsymbol{\tau}_0 = (d_0^2/D)a_2\lambda^3/a_1^2$ as the unit time, where a_1 = 0.8839 and a_2=0.6267, the dimensionless form of equation (3) can be simplified as:

$$a_s^2 \frac{\partial \phi}{\partial t} = [\phi - \lambda(u + Mc)(1-\phi^2)](1-\phi^2) + \nabla \cdot [a_s^2 \nabla \phi] + \frac{\partial}{\partial x}[|\nabla \phi|^2 a_s \frac{\partial a_s}{\partial \phi_x}] + \frac{\partial}{\partial y}[|\nabla \phi|^2 a_s \frac{\partial a_s}{\partial \phi_y}] \quad (5)$$

a_s is anisotropy function with $\vec{n} = -\nabla \phi / |\nabla \phi|$, the unit vector normal to the interface. $a_s(\vec{n}) = 1 + \varepsilon \cos(4\varphi)$ is commonly adopted to describe anisotropy in FCC crystal, where ε is a dimensionless anisotropy strength and $\varphi = \arctan(\partial_y \phi / \partial_x \phi)$ is normal direction of the interface. To simplify the calculation, the anisotropy function is usually written in the form of phase-field gradient. And it's also convenient to derivate the anisotropy function in 3-D space.

$$a_s = \left[1 - 3\varepsilon + 4\varepsilon \frac{(\partial \phi / \partial x)^4 + (\partial \phi / \partial y)^4}{|\nabla \phi|^4} \right] \quad (6)$$

The diffuse progress of the solute plays an important role in dendrite growth. It's complicated as a result of redistribution of solutes. We adopt the control equation proposed by Karma[9]:

$$\frac{(1+k) - \phi(1-k)}{2} \cdot \frac{\partial u}{\partial t} = \vec{\nabla} \cdot \left(D \cdot \frac{\phi}{2} \nabla u + \vec{j}_{at} \right) + \frac{1}{2} \frac{\partial \phi}{\partial t} \left(1 + (1-k)u \right) \quad (7)$$

D is dimensionless liquid diffusivity, solute diffusivity in the solid is ignored as solute transfer much slower. j_{at} is the anti-trapping current given by:

$$\vec{j}_{at} = \frac{1}{2\sqrt{2}} \left[1 + (1-k)u \right] \frac{\partial \phi}{\partial t} \frac{\nabla \phi}{|\nabla \phi|} \quad (8)$$

In equation (7) and (8), u is a dimensionless concentration defined as:

$$u = \frac{\dfrac{2c}{\left[1 + k - (1-k)\phi \right] c_\infty} - 1}{1-k} \quad (9)$$

2. Simulation and Results

A nucleus was embedded at the centre of the bottom in the calculation domain [see Figure 1], and the domain has a 1000x1600 mesh grid. Materials choice is succinonitrile because the availability of materials properties and it has the similar solidification behaviour as FCC metals [6]. The properties of the materials are listed in Table 1[7].

Table 1. Material properties of succinonitrile used in simulations

K	partition coefficient	0.15
d_0	capillary length (um)	0.035
E	anisotropy	0.04
D	liquid diffusivity(m^2/s)	2.0×10^{-8}s
$\|m\|C_0$	shift in the melting point (K)	2

In the calculation, λ (a coupling constant) was chosen as 6.3826, the grid spacing and time step $\Delta x = 0.4w_0$ and $\Delta t = 0.008\tau_0$. With the material properties of succinonitrile alloy, $\Delta x = 0.1$um, $\Delta t = 0.3\text{x}10^{-4}$s were used in simulations to maintain computational convergence.

In Figure 1 different colour represents different concentration level as indicated by the solute concentration scale bar. The left one was taken before the secondary arms appear, and in the right one there are many secondary dendrite arms, and the details will be analysed from different part of the domain in following sections.

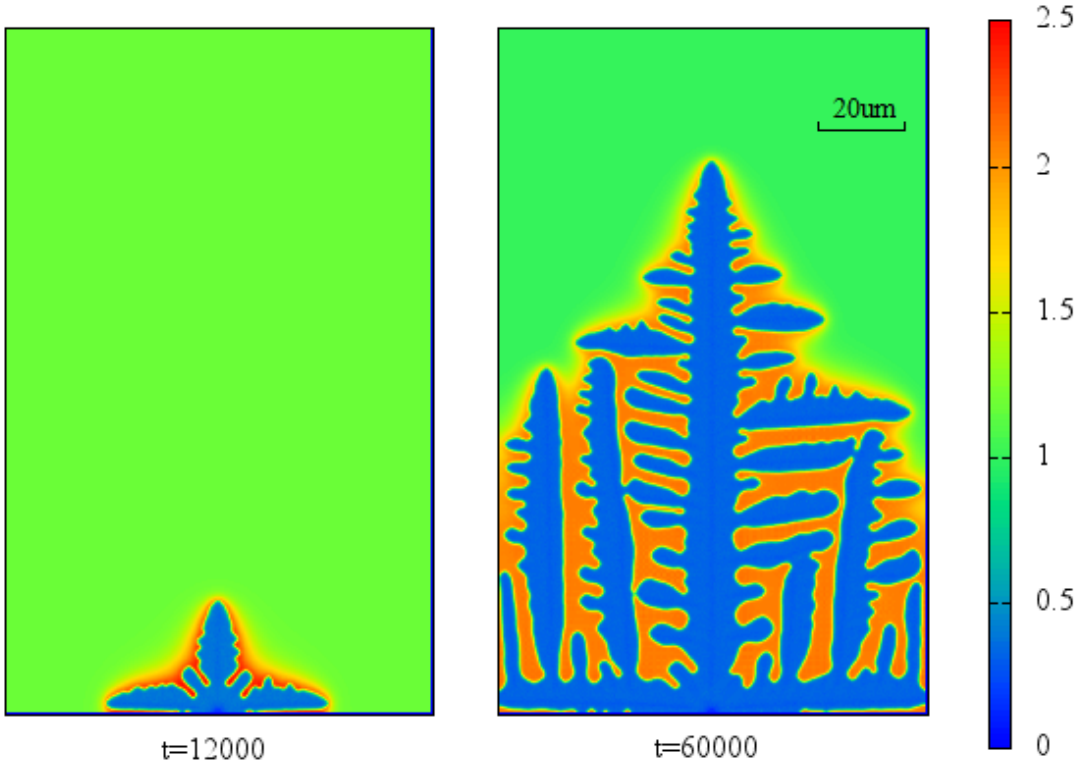

Figure 1. The concentration distribution c / c_0 at different time

2.1 The evolution of secondary arms

A typical growth process of a secondary arm in our simulations is shown in Figure 2. The growth of a secondary arm begins with a small fluctuation on the solid/liquid interface. In early stage, the tip of the arm grows like a parabola. But the base of the arm can't grow larger because of the enriched solute rejected from the solid-liquid interface, while the trunk of the arm increases continually if there is enough space. Then the arm becomes a fat arm trunk with a narrow root, which shows a similar morphology to the primary dendrite arm as shown in Figure 1 left. The length of the base and the area of the trunk for this secondary arm are plotted in Figure 3. In Figure 3 the length of the base (spacing) keeps invariant while the area increases almost linearly during the growth process.

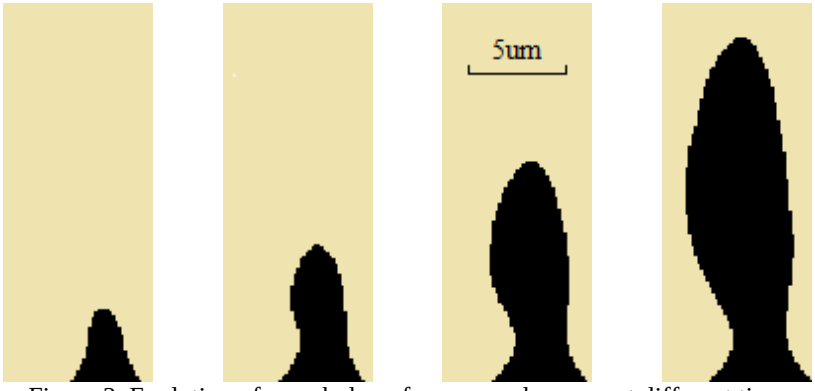

Figure 2. Evolution of morphology for a secondary arm at different time

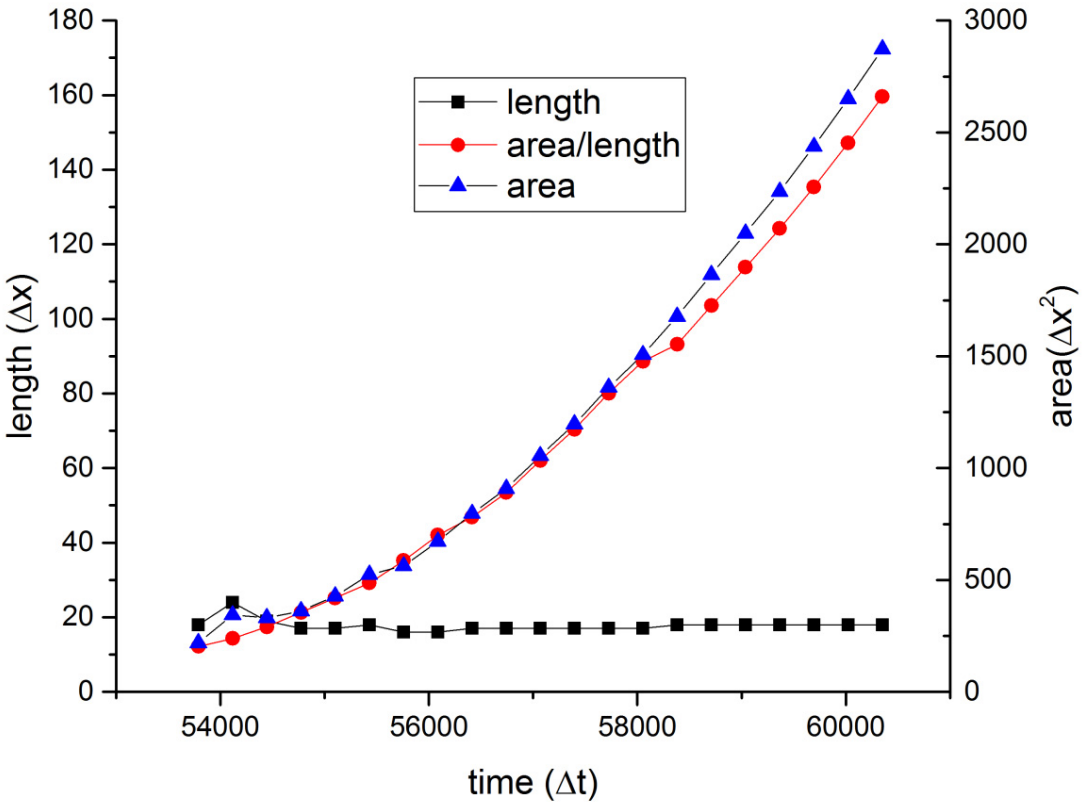

Figure 3. The evolution a secondary arms as a function of time (the blue lines is the area of the arm, black line is the length of the neck part. And the red line is the ratio of area and the length)

2.2 Remelting of secondary arms

If a FCC-structure equiaxed grain grows in a 2D domain, there will be only four primary dendrite arms in <001> directions. The angle between each adjacent arms is 90 degree. The adjacent secondary arms grow along one of the

<100> directions and spacing is getting narrower during growing. Prediction of solute interaction in secondary arms is challenging because the formation of secondary arms is not known before simulation and their growth condition is complicated. Different growth mechanisms were observed among secondary arms, some arms disappeared and some arms coalesced. Both of them were observed and the coarsening will be discussed here thoroughly. It shall be noted that flow in mesh zone during the growth of secondary arms was not included and it shall be of future work to investigate the effect of flow on the evolution of secondary arms.

The remelting of secondary arm is a consequence of the coarsening. This phenomenon has been observed in experiments both for succinonitrile[9] and metal alloys in real-time[10,11].

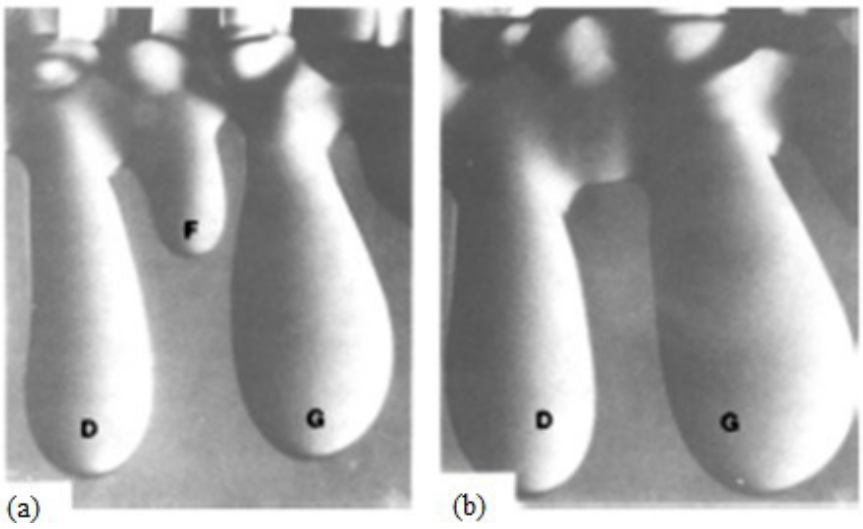

(a) and (b) remelting of a dendrite arm F in succinonitrile (secondary arm “F” disappears)[9]

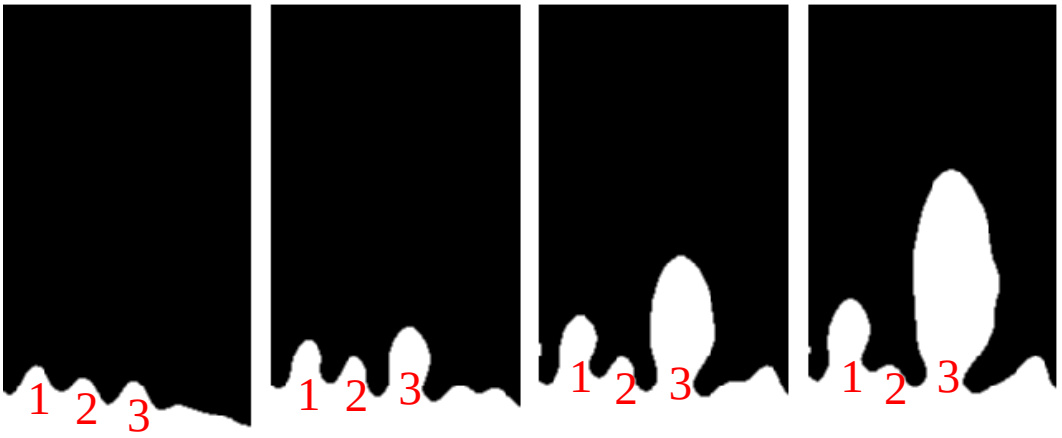

(c) remelting of arm 2 in phase-field simulation

Figure 4. The remelting of secondary arms (the primary dendrite arm grows from left to right.)

In our simulations, the remelting of secondary arm who fails in the competition with its neighbours is observed as in Figure 4(b). The primary dendrite arm grows from left to right. Three secondary arms appear near the tip of the primary arm, one by one, arm 1 appears the earliest while arm 3 appears the latest. Then all the three arms grow

from bottom to top. During the growth process, the arms reject solute, then the concentration is lower away from the arm tips. The tip of arm 1 is higher than arm 2, so the constitutional supercooling is larger in front of arm 1 than arm 2, and the arm 1 grows faster. For arm 3, because the concentration is lower near the tip of primary dendrite arm as we can see from Figure 1, it also gets a larger supercooling than arm 2. Both arm 1 and arm 3 grow faster than arm 2, then the solute rejected by them accumulates in front of arm 2. The higher solute concentration means the lower liquidus, when the liquidus falls lower than the local temperature, the arm 2 remelts until disappear.

2.3 Coarsening of secondary arms

Not all the competition between secondary arms can decide the winner. If the situation of two secondary arms is nearly the same, they will grow up together as Figure 5(a) left.

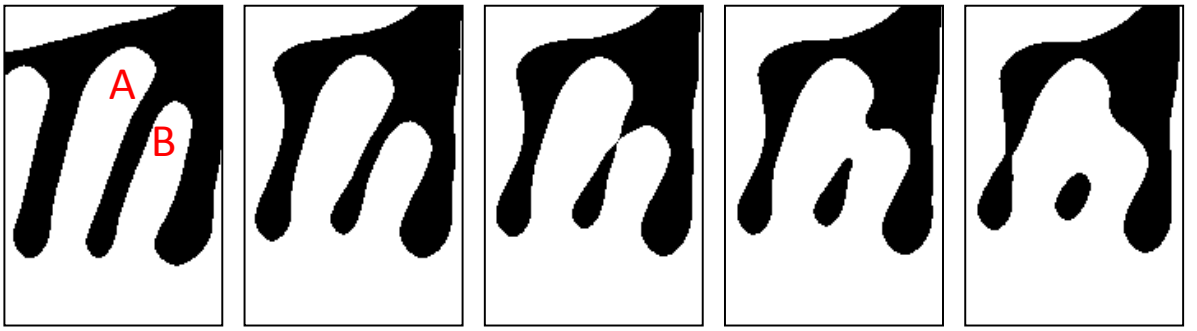

(a) Coarsening of secondary arms in phase-field simulation

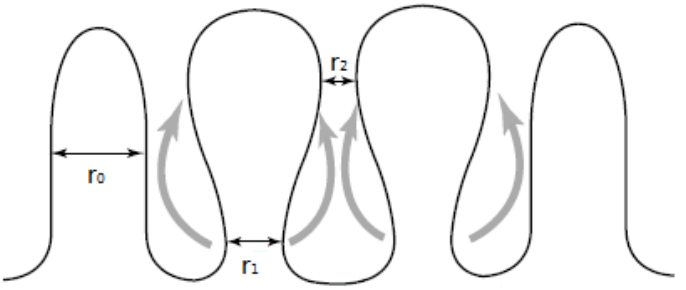

(b) Coarsening mechanism in adjacent arms[8]

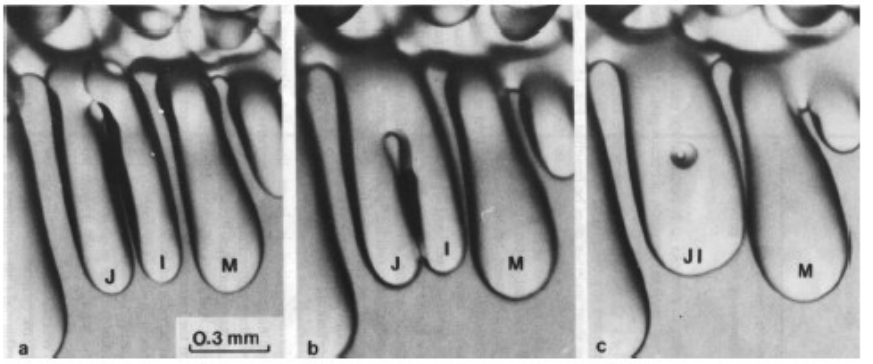

(c) merging of two secondary arms during solidification[9]

Figure 5 Coarsening of secondary dendrite arms during solidification

However in the later stage, the solute concentration outside the secondary arms is so high that the solute can hardly be rejected out and the arms grow slowly. Thereforeat the later stage of solidification the coarsening process plays the major role instead of growing. As shown in Figure 5(b)[8], the base of the arm r_2 will becomes narrower while the arm trunk becomes fatter, the spacing between two arms r_1 decreases until they reach each other to finish the solidification process.

3. Conclusion

A phase-field model coupled heat and solute diffusion was developed and applied to simulate the growth and coarsening of secondary arms for an FCC-structure equiaxed solidification. It is found that:

(1) The spacing of the secondary arms doesn't change as coarsening theory predicts, and keeps invariant when the arm grows into a steady state, but the volume of the secondary arms increases.
(2) Both remelting of secondary arms and coarsening of secondary arms were observed in the simulation, and predicted results agree well with the coarsening theory and experiment results.

Acknowledgements

This research is funded by National Natural Science Foundation of China (No. 51175292 and No. 513101062).

References

[1] Y. Xie, H. Dong, & J. Dantzig, Growth of Secondary Dendrite Arms of Fe C Alloy during Transient Directional Solidification by Phase-field Method. ISIJ INTERNATIONAL, 54(2), (2014), 430-436.

[2] Y. Xie, H. Dong, J. Liu, R. Davidchack, J. Dantzig, G. Duggan, D. Browne. A multi-scale approach to simulate solidification structure evolution and solute segregation in a weld pool. Journal of Algorithms and Computational Technology, 7(4), (2013), 489-507.

[3] Y. Xie, H. Dong, & J. Dantzig, Using the interface Peclet number to select the maximum simulation interface width in phase-field solidification modelling, Computational Materials Science 70 (2013) 71–76

[4] J.M.V. Quaresma, C.A. Santos, A. Garcia. Correlation between unsteady-state solidification conditions, dendrite spacings, and mechanical properties of Al-Cu alloys. Metallurgical and Materials Transactions A, 31(12), 2000, 3167-3178

[5] J.C. Ramirez, C. Beckermann, A. Karma. Phase-field modeling of binary alloy solidification with coupled heat and solute diffusion. Physical Review E, 69(2004), 051607

[6] J.D. Hunt, S.-Z. Lu. Numerical modeling of cellular/dendritic array growth: spacing and structure predictions. Metallurgical and Materials Transactions A ,27(3), 1996, 611-623

[7] A. Badillo, C. Beckermann. Phase-field simulation of the columnar-to-equiaxed transition in alloy solidification. Acta Materialia, 54(2006) 2015-2026

[8] D. Kammer, P.W. Voorhees. The morphological evolution of dendritic microstructures during coarsening. Acta Materialia, 54(2006) 1549-1558

[9] S.C. Huang and M.E. Glicksman. Fundamentals of dendritic solidification II:Development of sidebranch structure. Acta Metall. 29(1981),717–734

[10] N. Limodin, L. Salvo, E. Boller, In situ and real-time 3-D microtomography investigation of dendritic solidification in an Al–10 wt.% Cu alloy, Acta Materialia 57(2009) 2300-2310

[11] B. Li, H. D. Brody, A. Kazimirov. Real-time observation of dendrite coarsening in Sn-13%Bi alloy by synchrotron microradiography, PHYSICAL REVIEW E 70, 062602 (2004)